

Research Article

Synthesis, Characterization, and Relative Study on the Catalytic Activity of Zinc Oxide Nanoparticles Doped MnCO_3 , $-\text{MnO}_2$, and $-\text{Mn}_2\text{O}_3$ Nanocomposites for Aerial Oxidation of Alcohols

Mohamed E. Assal, Mufsir Kuniyil, Mohammed Rafi Shaik, Mujeeb Khan, Abdulrahman Al-Warthan, Mohammed Rafiq H. Siddiqui, and Syed Farooq Adil

Department of Chemistry, College of Science, King Saud University, P.O. Box 2455, Riyadh 11451, Saudi Arabia

Correspondence should be addressed to Syed Farooq Adil; sfakil@ksu.edu.sa

Received 27 March 2017; Revised 22 May 2017; Accepted 6 June 2017; Published 12 July 2017

Academic Editor: Mohamed Afzal Pasha

Copyright © 2017 Mohamed E. Assal et al. This is an open access article distributed under the Creative Commons Attribution License, which permits unrestricted use, distribution, and reproduction in any medium, provided the original work is properly cited.

Zinc oxide nanoparticles doped manganese carbonate catalysts [$X\% \text{ZnO}_x\text{-MnCO}_3$] (where $X = 0\text{--}7$) were prepared via a facile and straightforward coprecipitation procedure, which upon different calcination treatments yields different manganese oxides, that is, [$X\% \text{ZnO}_x\text{-MnO}_2$] and [$X\% \text{ZnO}_x\text{-Mn}_2\text{O}_3$]. A comparative catalytic study was conducted to evaluate the catalytic efficiency between carbonates and oxides for the selective oxidation of secondary alcohols to corresponding ketones using molecular oxygen as a green oxidizing agent without using any additives or bases. The prepared catalysts were characterized by different techniques such as SEM, EDX, XRD, TEM, TGA, BET, and FTIR spectroscopy. The $1\% \text{ZnO}_x\text{-MnCO}_3$ calcined at 300°C exhibited the best catalytic performance and possessed highest surface area, suggesting that the calcination temperature and surface area play a significant role in the alcohol oxidation. The $1\% \text{ZnO}_x\text{-MnCO}_3$ catalyst exhibited superior catalytic performance and selectivity in the aerial oxidation of 1-phenylethanol, where 100% alcohol conversion and more than 99% product selectivity were obtained in only 5 min with superior specific activity ($48 \text{ mmol}\cdot\text{g}^{-1}\cdot\text{h}^{-1}$) and 390.6 turnover frequency (TOF). The specific activity obtained is the highest so far (to the best of our knowledge) compared to the catalysts already reported in the literatures used for the oxidation of 1-phenylethanol. It was found that ZnO_x nanoparticles play an essential role in enhancing the catalytic efficiency for the selective oxidation of alcohols. The scope of the oxidation process is extended to different types of alcohols. A variety of primary, benzylic, aliphatic, allylic, and heteroaromatic alcohols were selectively oxidized into their corresponding carbonyls with 100% convertibility without overoxidation to the carboxylic acids under base-free conditions.

1. Introduction

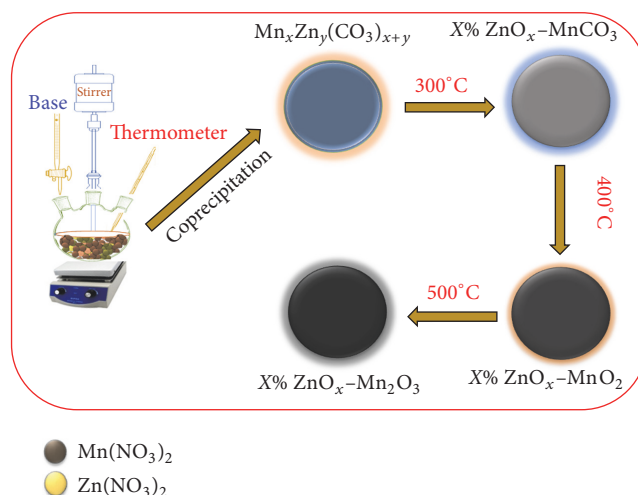
Selective catalytic oxidation of alcohols to corresponding carbonyl compounds is one of the most pivotal functional group transformations in organic chemistry [1–6]. The oxidation products such as aldehyde and ketone derivatives are important precursors and intermediates in the cosmetics, perfumery, flame-retardants, insecticides, confectionary, biofuels, and pharmaceutical industries [7–11]. Usually, conventional oxidation of alcohols was conducted using toxic and expensive stoichiometric oxidizing agents such as CrO_3 , KMnO_4 , NaClO , $\text{Na}_2\text{Cr}_2\text{O}_7$, SeO_2 , and Br_2 and leads to

producing harmful by-products [12, 13]. In contrast, using clean and low cost oxidizing agents, such as aqueous hydrogen peroxide and particularly molecular oxygen to produce water, is the only side product and has gained growing interest from the sustainable and green chemistry point of views [14, 15]. In this context, noble metals such as gold [16–20], palladium [21], platinum [22–24], ruthenium [25, 26], and rhodium [27, 28] have been used as a heterogeneous catalyst for the alcohol oxidation with high catalytic activities and selectivities. Beside their high costs, these precious metals also have serious toxicity issues and difficulty in preparation and rarity of these noble metals makes these catalysts

impractical for industrial applications [29, 30]. Therefore, huge efforts have been made in order to replace these expensive noble metal catalysts with cheaper and plentiful nonnoble metals, for example, copper [31, 32], cobalt [33, 34], nickel [35–37], iron [38, 39], vanadium [40], silver [41, 42], chromium [43], molybdenum [44, 45], rhenium [46], and zirconium [47], for selective oxidation of alcohols. The metal, metal oxide, and mixed metal oxide nanoparticles catalysts were also found to be highly effective for the catalytic oxidation of alcohols. In addition, it has been widely reported that the catalytic activity of mixed metal oxide nanoparticles catalysts was remarkably enhanced upon doping with other metals, maybe because the metal nanoparticles possess huge surface area [48, 49].

Manganese carbonate (MnCO_3) has been considered one of the inexpensive and most stable metal oxides with high catalytic performance. Because MnCO_3 has various leads such as being most active, being stable, having low cost, and being environmental friendly catalyst, MnCO_3 and manganese oxides have been widely castoff as a catalyst or catalyst support for the catalytic oxidation of alcohols into carbonyls [50–53]. Moreover, it has several features, such as being highly active, stable, inexpensive, and ecofriendly catalyst [51–56]. However, different types of manganese oxide, mixed manganese oxide, and noble metal doped/supported Mn oxides were widely employed for the catalytic oxidation of numerous organic substrates, for instance, oxidation of naphthalene to carbon dioxide [57], oxidation of carbon monoxide to CO_2 [58, 59], oxidation of toluene to CO_2 [60], oxidation of ethylene and propylene to CO_2 [61], oxidation of cyclohexane to cyclohexanol and cyclohexanone [62], oxidation of alkyl aromatics to ketones [63], oxidation of 4-tert-butyltoluene to 4-tert-butylbenzaldehyde [64], and oxidation of formaldehyde to CO_2 [65].

In continuation of our efforts on the use of different mixed metal oxide nanoparticles as an efficient catalyst for the selective oxidation of alcohols in presence of molecular O_2 [18, 32, 41, 48, 49], we demonstrate herein a facile and straightforward procedure for the preparation of ZnO_x NPs doped manganese carbonates or oxides employed for oxidation of secondary alcohols with environmentally friendly oxidizing agent such molecular O_2 which produces water as the only by-product under base-free conditions. The reaction circumstances have been optimized with different weight percentages of ZnO_x , reaction times, calcination temperatures, reaction temperatures, and catalyst amounts using oxidation of 1-phenylethanol into acetophenone as a reaction model. The as-prepared catalyst was employed for oxidation of different types of alcohols. It was found that most of alcohols that were used in this study were completely converted to their corresponding aldehydes or ketones in extremely short reaction time without overoxidation to the acids. Moreover, the prepared catalysts have been characterized by several types of techniques, like scanning electron microscopy (SEM), energy dispersive X-ray spectroscopy (EDX), X-ray diffraction (XRD), transmission electron microscopy (TEM), Fourier transform infrared spectroscopy (FTIR), thermogravimetric analysis (TGA), and Brunauer-Emmett-Teller (BET) surface area measurement spectroscopies.



SCHEME 1: Graphical illustration of the synthesis of the $X\% \text{ZnO}_x\text{-MnCO}_3$ oxide and other products formed.

2. Experimental Section

2.1. Preparation of the Catalysts. ZnO_x NPs doped MnCO_3 catalysts of the type $X\% \text{ZnO}_x\text{-MnCO}_3$ (where $X = 0, 1, 3, 5$, and 7) were prepared by coprecipitation method where $\% X$ denotes w/w%. Stoichiometric amount of manganese (II) nitrate tetrahydrate ($\text{Mn}(\text{NO}_3)_2 \cdot 4\text{H}_2\text{O}$) and zinc nitrate hexahydrate ($\text{Zn}(\text{NO}_3)_2 \cdot 6\text{H}_2\text{O}$) was dissolved in distilled water. About 100 mL of the mixture of solutions was taken in a glass three-necked round-bottom flask. The resulting mixture was heated to 80°C , while stirring using a mechanical stirrer and 0.5 M solution of sodium hydrogen carbonate (NaHCO_3) was added dropwise until the solution attained a pH 9. The solution was continued to stir at the same temperature for about 3 hours and then left on stirring over night at room temperature. The solution was filtered by centrifugation and the solid product obtained was dried at 70°C overnight; this upon calcination at different temperatures yielded different catalysts, which were used for comparative study of catalytic properties. A pictorial illustration is given in Scheme 1.

2.2. Characterization Techniques. Scanning electron microscopy (SEM) and elemental analysis (energy dispersive X-ray analysis: EDX) were carried out using Jeol SEM model JSM 6360A (Japan). This was used to determine the morphology of nanoparticles and its elemental composition. Fourier transform infrared (FTIR) spectra were registered on a Perkin-Elmer 1000 FTIR instrument (Waltham, MA, USA); the samples were prepared in KBr pellets. Transmission electron microscopy (TEM) was carried out using Jeol TEM model JEM-1101 (Japan), which was used to determine the shape and size of nanoparticles. Powder X-ray diffraction studies were carried out using Altima IV [Make: Regaku] X-ray diffractometer. BET surface area was measured on a NOVA 4200e surface area and pore size analyzer. Thermogravimetric analysis was carried out using Perkin-Elmer Thermogravimetric Analyzer 7.

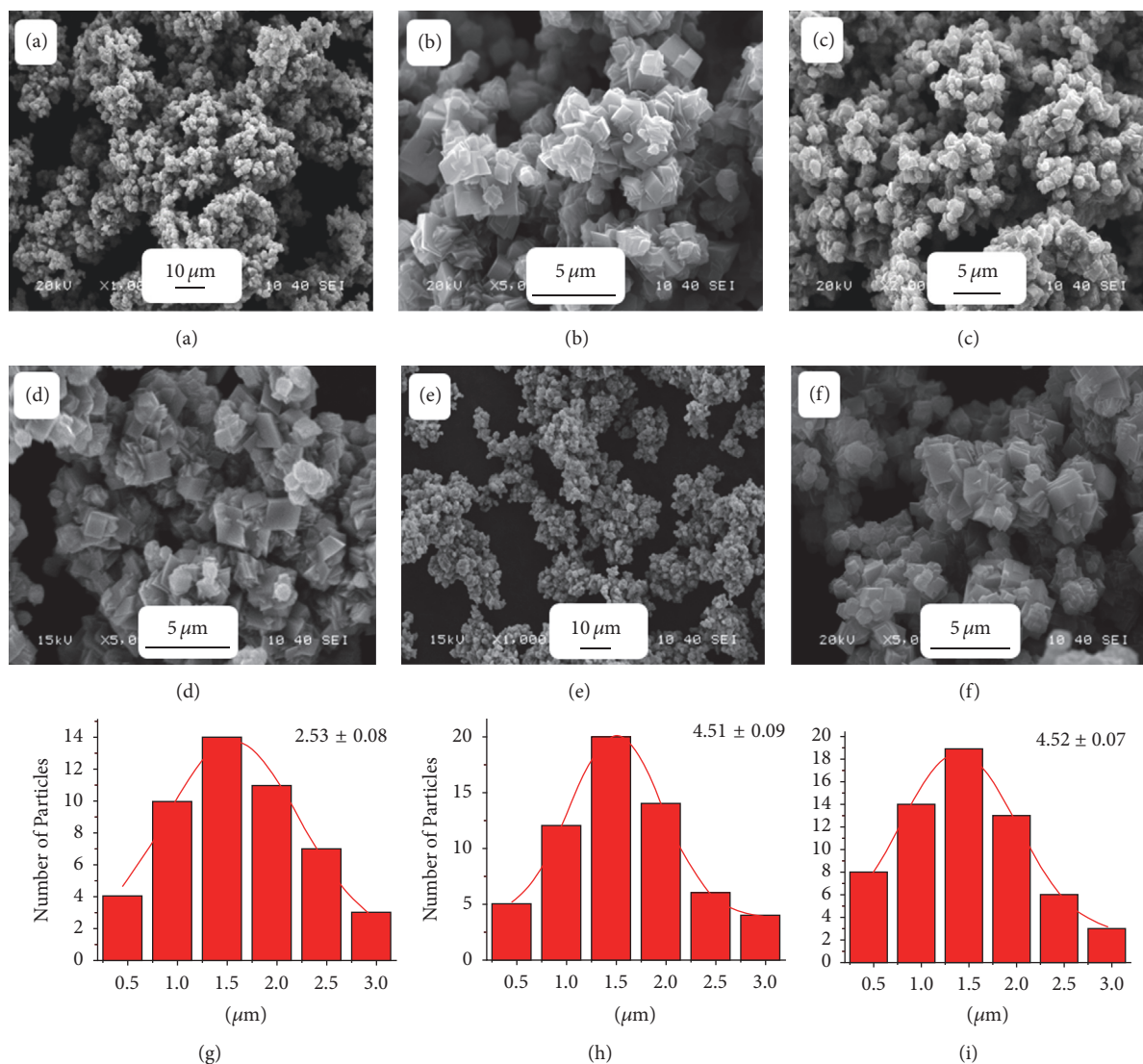


FIGURE 1: SEM analysis of the catalysts calcined at (a)-(b) 300°C; (c)-(d) 400°C; (e)-(f) 500°C; (a)-(b) overview image for as-prepared 1% ZnO_x-MnCO₃; (c)-(d) overview image of 1% ZnO_x-MnO₂; (e)-(f) overview image of 1% ZnO_x-Mn₂O₃; (g) particle size distribution of 1% ZnO_x-MnCO₃; (h) particle size distribution of 1% ZnO_x-MnO₂; (i) particle size distribution of 1% ZnO_x-Mn₂O₃.

2.3. Typical Procedure for Alcohol Oxidation. Liquid-phase oxidation of 1-phenylethanol was performed in glass flask equipped with a magnetic stirrer, reflux condenser, and thermometer. In a typical experiment, a mixture of the 1-phenylethanol (2 mmol), toluene (10 mL), and the catalyst (0.3 g) was transferred in a glass three-necked round-bottomed flask (100 mL); the resulting mixture was then heated to desired temperature with vigorous stirring. The oxidation experiment was started by bubbling oxygen gas at a flow rate of 20 mL/min into the reaction mixture. After the reaction, the solid catalyst was filtered off by centrifugation and the liquid products were analyzed by gas chromatography to determine the conversion of the alcohol and product selectivity by GC, 7890A, Agilent Technologies Inc., equipped with a flame ionization detector (FID) and a 19019S-001 HP-PONA column.

3. Results and Discussion

3.1. Characterization of the Catalysts. The as-synthesized catalysts surface morphology was analyzed by using scanning electron microscopy (SEM). The SEM images of the as-synthesized catalysts calcined at different temperatures, 1% ZnO_x-MnCO₃ at 300°C, 1% ZnO_x-MnO₂ at 400°C, and 1% ZnO_x-Mn₂O₃ at 500°C, exhibited morphology as shown in Figures 1(a)–1(e). The SEM image of the catalysts discloses well defined and spherical shaped morphology. Furthermore, it is observed that the morphology of the catalysts did not vary with the different calcination temperatures but it varies with size of the particles; as the calcination temperature increases ZnO_x NPs size increases and also the spherical shaped morphology of all the catalysts clearly exhibited in Figures 1(a)–1(e). The particle size distribution of SEM micrographs

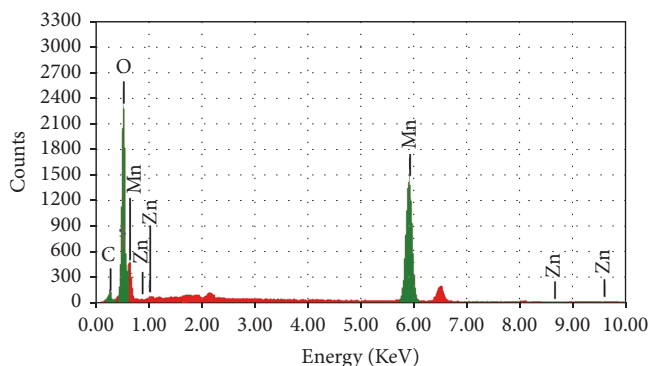


FIGURE 2: EDX analysis of the as-synthesized catalysts calcined 1% $\text{ZnO}_x\text{-MnCO}_3$.

of the as-synthesized catalysts, 1% $\text{ZnO}_x\text{-MnCO}_3$ calcined at different temperatures, 1% $\text{ZnO}_x\text{-MnCO}_3$ at 300°C, 1% $\text{ZnO}_x\text{-MnO}_2$ at 400°C, and 1% $\text{ZnO}_x\text{-Mn}_2\text{O}_3$ at 500°C, was assessed by using the program software J as shown in Figures 1(g)–1(i). The particle size was found to be approximately equal to 2.53, 4.51, and 4.79 μm in the catalyst precalcined at 300, 400, and 500°C correspondingly. From the attained results, it is noticed that while there is a variation in particle sizes among the precalcined catalysts 1% $\text{ZnO}_x\text{-MnCO}_3$ at 300°C and 1% $\text{ZnO}_x\text{-MnO}_2$ at 400°C, there is a merely small difference in the particle sizes among the precalcined catalysts 1% $\text{ZnO}_x\text{-MnO}_2$ at 400°C and 1% $\text{ZnO}_x\text{-Mn}_2\text{O}_3$ at 500°C.

3.2. Energy Dispersive X-Ray Spectroscopy (EDX) Analysis. The elemental composition of the catalyst 1% $\text{ZnO}_x\text{-MnCO}_3$ at 300°C was investigated using energy dispersive X-ray spectroscopy (EDX). The intense signal at 5.5–6 keV strongly recommends that “Mn” was the major element, which has an optical absorption in this range due to the surface plasmon resonance (SPR). The signals at 0.8, 1.1, 8.6, and 9.6 strongly endorse that “Zn” was the element. It was also prominent that the other signals were also attained in the range 0.0–0.5 keV which denotes the typical absorption of carbon and oxygen. The found values of composition percentage of the Zn, Mn, and O_2 present in the catalyst were nearly identical to the values of the composition castoff in preparing the catalyst shown in Figure 2.

3.3. X-Ray Diffraction (XRD) Analysis. The as-prepared catalysts crystal structure was analyzed by using X-ray diffraction (XRD). The XRD images of the catalysts 1% $\text{ZnO}_x\text{-MnCO}_3$ uncalcined and calcined at different temperatures, 1% $\text{ZnO}_x\text{-MnCO}_3$ at 300°C, 1% $\text{ZnO}_x\text{-MnO}_2$ at 400°C, and 1% $\text{ZnO}_x\text{-Mn}_2\text{O}_3$ at 500°C are shown in Figure 3. The found diffraction signals confirmed that as-synthesized catalysts are in crystalline nature. The calcined catalysts conceded various phases of manganese oxide alongside with the traces of ZnO_x . The uncalcined catalyst shows patterns which were obtained to be in agreement with the standard XRD data of rhodochrosite syn- MnCO_3 (JCPDS number 44-1472). With the calcination at 300°C the XRD pattern exhibits the existence of rhodochrosite D- MnCO_3 (JCPDS number

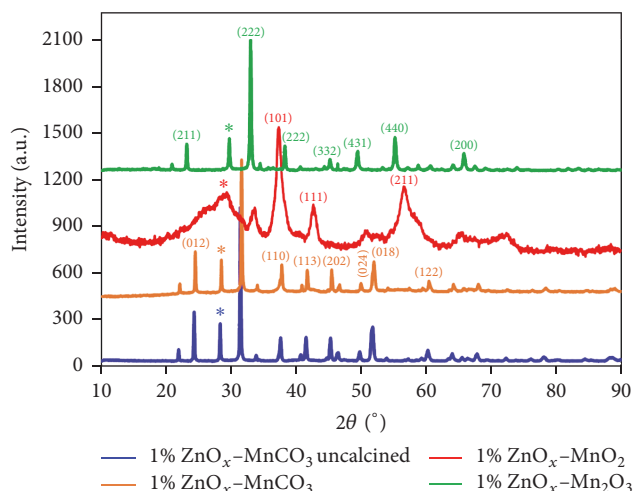


FIGURE 3: XRD pattern of the catalyst 1% $\text{ZnO}_x\text{-MnCO}_3$ uncalcined and catalyst calcined at different temperatures 1% $\text{ZnO}_x\text{-MnCO}_3$; 1% $\text{ZnO}_x\text{-MnO}_2$; and 1% $\text{ZnO}_x\text{-Mn}_2\text{O}_3$.

1-0981). Subsequently when the calcination temperature was further increased to 400°C the XRD spectra attained were in agreement with pyrolusite MnO_2 (JCPDS number 24-0735). When the catalyst was calcined at 500°C the XRD pattern obtained was in agreement with bixbyite- Mn_2O_3 (JCPDS number 2-0909). The reflections noticed with symbol asterisk (*) might be owing to the occurrence of ZnO_x . The as-synthesized nanocomposite catalysts have been matched with known compounds stated in the literature.

3.4. Fourier Transform Infrared Spectroscopy (FTIR) Analysis. The FTIR spectrum was used to classify the functional groups on the surface of the as-synthesized catalyst. The FTIR spectra of the catalysts at different calcination temperatures (300, 400, and 500°C), that is, 1% $\text{ZnO}_x\text{-MnCO}_3$, 1% $\text{ZnO}_x\text{-MnO}_2$, and 1% $\text{ZnO}_x\text{-Mn}_2\text{O}_3$, correspondingly are displayed in Figure 4. High wavenumber zone displays stretching vibrations of the surface hydroxyl group and physisorbed water. The characteristic bands of νOH located around 3475 cm^{-1} were found to be in the 300, 400, and 500°C calcined catalyst. The intensity of these bands decreases as the calcination temperature increase demonstrates the decrease of the existence of OH group and H_2O on the catalyst surface. The absorption band at around 1635 cm^{-1} resembles fingerprint bending vibration modes of hydroxyl groups [83]. Therefore, it can be said that OH group in the catalyst surface acts a significant part in the 1-phenylethanol oxidation, in which the 1% $\text{ZnO}_x\text{-MnCO}_3$ catalyst displays the highest catalytic performance associated with the other calcination temperatures [84]. In case of 300°C calcination temperature, the presence of a sharp peak at nearly 1356 cm^{-1} is a fingerprint for surface carbonate (CO_3^{2-}) group which confirmed the occurrence of carbonate group in the surface of the catalyst and these results are in good agreement with EDX and XRD results [85, 86]. In case of 400 and 500°C, that is, 1% $\text{ZnO}_x\text{-MnO}_2$ and 1% $\text{ZnO}_x\text{-Mn}_2\text{O}_3$ correspondingly, the absorption peak

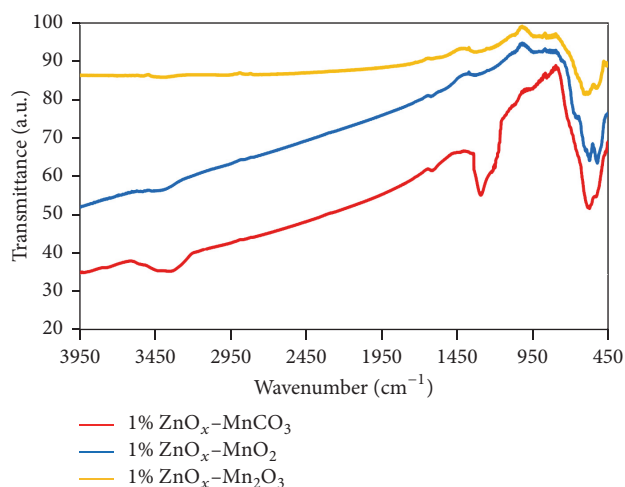
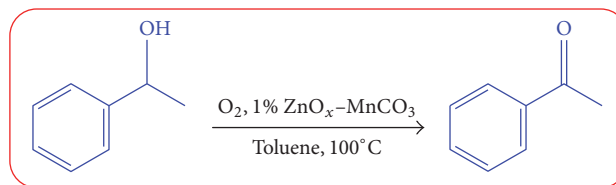


FIGURE 4: FTIR spectra of the catalyst calcined at different temperatures 1% $\text{ZnO}_x\text{-MnCO}_3$; 1% $\text{ZnO}_x\text{-MnO}_2$; and 1% $\text{ZnO}_x\text{-Mn}_2\text{O}_3$.

at around 1356 cm^{-1} representing carbonate group almost disappears, maybe owing to manganese carbonate converted to manganese oxides at elevated temperature. Sharp peaks are attained in the range of $520\text{--}610\text{ cm}^{-1}$ typical for different oxides of manganese [87, 88].

3.5. High-Resolution Transmission Electron Microscopy (HRTEM) Analysis. The HRTEM images of catalysts calcined at different temperatures, 1% $\text{ZnO}_x\text{-MnCO}_3$ at 300°C , 1% $\text{ZnO}_x\text{-MnO}_2$ at 400°C , and 1% $\text{ZnO}_x\text{-Mn}_2\text{O}_3$ at 500°C , are displayed in Figures 5(a)–5(c). Moreover, the HRTEM image reveals that the calcination temperature plays significant role in particle size. The particles size and agglomeration of the as-synthesized catalyst increase with increase of calcination temperature. It might also be owing to the decomposition of MnCO_3 to manganese oxide. The interplanar distance estimated from the HRTEM image of the catalysts calcined at 300°C (Figure 5(a)) revealed d -spacing of 0.29 nm and 0.23 nm resembles the (104) and the (110) planes of rhombohedral MnCO_3 . The sample calcined at 400°C revealed d -spacing of 0.25 nm resembled the (201) planes of MnO_2 (Figure 5(b)). For the sample calcined at 500°C (Figure 5(c)), the most noticeable lattice spacing resembles the (200) plane of $\alpha\text{-Mn}_2\text{O}_3$.

3.6. Thermal Gravimetric Analysis. For the as-synthesized catalyst calcined at different temperatures, 1% $\text{ZnO}_x\text{-MnCO}_3$ at 300°C , 1% $\text{ZnO}_x\text{-MnO}_2$ at 400°C , and 1% $\text{ZnO}_x\text{-Mn}_2\text{O}_3$ at 500°C , thermal stability was investigated by thermogravimetric analysis (TGA) as displayed in Figure 6. The thermogram of the as-synthesized catalyst calcined at 300°C demonstrates that the catalyst is steady up to 415°C with very insignificant percentage of weight loss that is less than 3%, due to the exclusion of volatile surface-absorbed water and volatile impurities. The highest loss of weight percentage was noticed by nearly 10%–12% in the temperature range of about $420\text{--}600^\circ\text{C}$ which appears to be due to the loss of CO_2 of MnCO_3 to form MnO_2 and further oxidation of



SCHEME 2: Aerial oxidation of 1-phenylethanol into acetophenone.

MnO_2 to Mn_2O_3 as indicated from the literature by Zhu et al. [89]. When the temperature is increased up to 800°C , the highest weight loss is noticed around 14%. Furthermore, the as-synthesized catalyst calcined at 400°C exhibited the maximum total weight loss percentage around 9% when the catalyst was heated up to 800°C , whereas in the case of the catalyst calcined at 500°C it displayed weight loss percentage of around 4%. Consequently, the catalysts displayed a thermal stability up to around 415°C and a marginally thermal stability decrease attained with raise in temperature.

3.7. Surface Area Measurements. The surface area of the as-synthesized catalysts was studied using BET surface area analysis, in order to determine the surface area and to understand the relationship between surface area and catalytic activity of the as-prepared catalyst for the oxidation of 1-phenylethanol. Table 1 displayed that the specific surface area of the prepared catalyst calcined at different calcination temperature such as 300°C , 400°C , and 500°C , that is, 1% $\text{ZnO}_x\text{-MnCO}_3$, 1% $\text{ZnO}_x\text{-MnO}_2$, and 1% $\text{ZnO}_x\text{-Mn}_2\text{O}_3$, respectively, was about 120.26 , 69.83 , and $21.79\text{ m}^2\cdot\text{g}^{-1}$, respectively. It can be observed that the catalyst with composition 1% $\text{ZnO}_x\text{-MnCO}_3$ calcined at 300°C has higher specific surface area than the catalyst obtained by calcining the prepared material at higher temperatures, that is, 400°C and 500°C . The results obtained suggest that at higher calcination temperatures there is a decrease in the surface area due to the sintering. Thus, this may partially be responsible for high catalytic performance in case of the catalyst calcined at 300°C , while in case of 400 and 500°C calcination treatment, there is a considerable decrease in the specific surface area, maybe due to agglomeration of ZnO_x NPs, which has negative effect on the catalyst functioning, which leads to poor alcohol conversion. From the above findings, it can be said that both calcination treatment and the surface area of the synthesized catalyst play a crucial role in the surface area of the synthesized catalyst, which in turn affects the working of the catalyst.

3.8. Catalytic Evaluation. In order to get effective results, the various parameters such as various percentages weight of ZnO_x , reaction time, calcination temperature, catalyst amount, and reaction temperature were optimized as shown in Tables 1–4. For this purpose, the oxidation of 1-phenylethanol was chosen as a substrate model (Scheme 2).

3.8.1. Influence of Calcination Temperature. The effect of calcination temperature on the oxidation of 1-phenylethanol

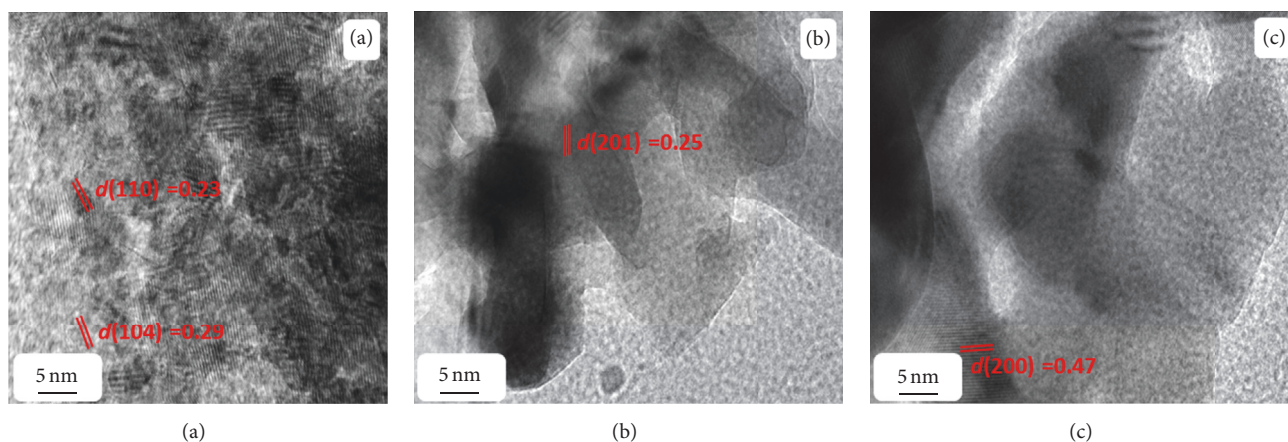


FIGURE 5: The HRTEM images of catalyst calcined at different temperatures: (a) 1% $\text{ZnO}_x\text{-MnCO}_3$; (b) 1% $\text{ZnO}_x\text{-MnO}_2$; and (c) 1% $\text{ZnO}_x\text{-Mn}_2\text{O}_3$.

TABLE 1: Catalytic oxidation of 1-phenylethanol in different calcination temperatures of the prepared catalysts.^[a]

Entry	Catalyst	T ($^{\circ}\text{C}$)	SA ($\text{m}^2 \text{g}^{-1}$)	Conv. (%)	Sp. activity ($\text{mmol}\cdot\text{g}^{-1}\cdot\text{h}^{-1}$)	TON	TOF (h^{-1})	Sel. (%)
1	1% $\text{ZnO}_x\text{-MnCO}_3$	300	120.26	100.00	22.22	54.25	180.83	>99
2	1% $\text{ZnO}_x\text{-MnO}_2$	400	69.83	81.49	18.11	44.21	147.37	>99
3	1% $\text{ZnO}_x\text{-Mn}_2\text{O}_3$	500	21.79	55.94	12.43	30.35	101.16	>99

^[a] Reaction conditions: 2 mmol of 1-phenylethanol, 300 mg of catalyst, oxygen with rate 20 mL/min, reaction temperature at 100°C , 10 mL of toluene, and 18 min of reaction time.

TABLE 2: Effect of different weight % of ZnO_x on the 1-phenylethanol oxidation.^[a]

Entry	Catalyst	Conv. (%)	Sp. activity ($\text{mmol}\cdot\text{g}^{-1}\cdot\text{h}^{-1}$)	TON	TOF (h^{-1})	Sel. (%)
1	0% $\text{ZnO}_x\text{-MnCO}_3$	78.31	17.40	/	/	>99
2	1% $\text{ZnO}_x\text{-MnCO}_3$	100.00	22.22	54.25	180.83	>99
3	3% $\text{ZnO}_x\text{-MnCO}_3$	92.43	20.54	18.08	60.27	>99
4	5% $\text{ZnO}_x\text{-MnCO}_3$	72.29	16.06	10.85	36.17	>99
5	7% $\text{ZnO}_x\text{-MnCO}_3$	60.14	13.36	7.70	25.67	>99

^[a] Reaction conditions: 2 mmol of 1-phenylethanol, 300 mg of catalyst, calcination temperature at 300°C , oxygen with rate 20 mL/min, reaction temperature at 100°C , 10 mL of toluene, and 18 min of reaction time.

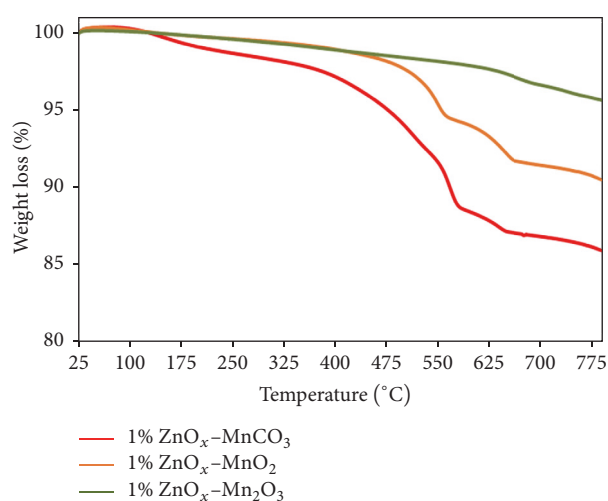


FIGURE 6: TGA of as-synthesized catalyst calcined at different calcination temperatures 300°C , 400°C , and 500°C ; 1% $\text{ZnO}_x\text{-MnCO}_3$; 1% $\text{ZnO}_x\text{-MnO}_2$; and 1% $\text{ZnO}_x\text{-Mn}_2\text{O}_3$.

has been examined. The synthesized catalyst calcined at different temperatures such as 300°C , 400°C , and 500°C . The catalysts showed high product selectivity during all oxidation experiments (above 99%). Notwithstanding the oxidation of 1-phenylethanol is strongly affected by calcination temperature. The obtained results concluded that the applied calcination treatment has a marked inhibiting effect on the oxidation process by decreasing the alcohol conversion [90, 91]. For example, the catalyst calcined at 300°C , that is, 1% $\text{ZnO}_x\text{-MnCO}_3$, exhibits the highest alcohol conversion (100%) along with $22.22 \text{ mmol}\cdot\text{g}^{-1}\cdot\text{h}^{-1}$ specific activity and 180.83 h^{-1} TOF, within 18 min of the reaction (Table 1, entry 1), while catalysts calcined at 400 and 500°C , that is, 1% $\text{ZnO}_x\text{-MnO}_2$ and 1% $\text{ZnO}_x\text{-Mn}_2\text{O}_3$, respectively, gave a lower conversion of 81.49% and 55.94%, respectively, under similar circumstances (Table 1, entries 2, 3). It is worth mentioning that these observations correlate with the BET surface area results of the prepared catalyst. 1% $\text{ZnO}_x\text{-MnCO}_3$, 1% $\text{ZnO}_x\text{-MnO}_2$, and 1% $\text{ZnO}_x\text{-Mn}_2\text{O}_3$ were 120.26, 69.83, and

TABLE 3: Effect of reaction temperature on the oxidation of 1-phenylethanol using 1% $\text{ZnO}_x\text{-MnCO}_3$ as the catalyst.^[a]

Entry	T ($^{\circ}\text{C}$)	Conv. (%)	Sp. activity ($\text{mmol}\cdot\text{g}^{-1}\cdot\text{h}^{-1}$)	TON	TOF (h^{-1})	Sel. (%)
1	20	36.07	8.01	19.57	65.23	>99
2	40	52.84	11.74	28.67	95.57	>99
3	60	69.12	15.36	37.50	125.0	>99
4	80	84.69	18.82	45.94	153.13	>99
5	100	100.0	22.22	54.25	180.83	>99

^[a] Reaction conditions: 2 mmol of 1-phenylethanol, 300 mg of catalyst, calcination temperature at 300°C , oxygen with rate 20 mL/min, 10 mL of toluene, and 18 min of reaction time.

TABLE 4: The effect of the catalyst 1% $\text{ZnO}_x\text{-MnCO}_3$ amount on the catalytic efficiency.^[a]

Entry	Catalyst amount (mg)	Conv. (%)	Sp. activity ($\text{mmol}\cdot\text{g}^{-1}\cdot\text{h}^{-1}$)	TON	TOF (h^{-1})	Sel. (%)
1	100	40.58	97.39	66.05	792.60	>99
2	200	56.13	67.36	45.67	548.04	>99
3	300	70.98	56.78	38.51	462.12	>99
4	400	86.01	51.61	34.96	419.52	>99
5	500	100	48.0	32.55	390.6	>99

^[a] Reaction conditions: 2 mmol of 1-phenylethanol, calcination temperature at 300°C , oxygen with rate 20 mL/min, reaction temperature at 100°C , 10 mL of toluene, and 5 min of reaction time.

$21.79\text{ m}^2\cdot\text{g}^{-1}$, respectively. As we mentioned, the prepared catalyst 1% $\text{ZnO}_x\text{-MnCO}_3$ exhibited the highest alcohol conversion and possessed the highest surface area among all other calcination temperatures. In contrast, the catalyst calcined at 400, that is, 1% $\text{ZnO}_x\text{-MnO}_2$, and 500°C , that is, 1% $\text{ZnO}_x\text{-Mn}_2\text{O}_3$, provided lesser activity and lower surface area. Therefore, it can be deduced that the catalytic activity is strongly influenced by calcination temperature of the catalyst. So we chose to use the catalyst calcined at 300°C , that is, 1% $\text{ZnO}_x\text{-MnCO}_3$, as the best calcination temperature to optimize other parameters. The results including 1-phenylethanol conversion, surface area, specific activity, turnover number (TON), turnover frequency (TOF), and acetophenone selectivity over the prepared catalyst were summarized in Table 1 and plotted in Figure 7.

3.8.2. Influence of the Amount of ZnO_x Promotor. In order to get the best catalytic performance, the influence of % ZnO_x on the reaction yield was studied by varying load of ZnO_x on MnCO_3 support ranging from 0 to 7% and the graphical representation of the results has been shown in Figure 8 and listed in Table 2. The results showed that undoped MnCO_3 catalyst, that is, 0% $\text{ZnO}_x\text{-MnCO}_3$, gives about 78.31% conversion of 1-phenylethanol along with specific activity of $17.40\text{ mmol}\cdot\text{g}^{-1}\cdot\text{h}^{-1}$ within 18 min (Table 2, entry 1). However, after ZnO_x NPs doping on MnCO_3 , the catalytic efficiency has been remarkably enhanced, where the 1% $\text{ZnO}_x\text{-MnCO}_3$ catalyst exhibits a full alcohol conversion under identical reaction conditions and the calculated specific activity was found to be $22.22\text{ mmol}\cdot\text{g}^{-1}\cdot\text{h}^{-1}$ and 180.83 h^{-1} TOF (Table 2, entry 2), whereas as the weight percentage of ZnO_x is further increased, the catalysts 3% $\text{ZnO}_x\text{-MnCO}_3$, 5% $\text{ZnO}_x\text{-MnCO}_3$, and 7% $\text{ZnO}_x\text{-MnCO}_3$ provided a lower alcohol conversion of 92.43, 72.29, and

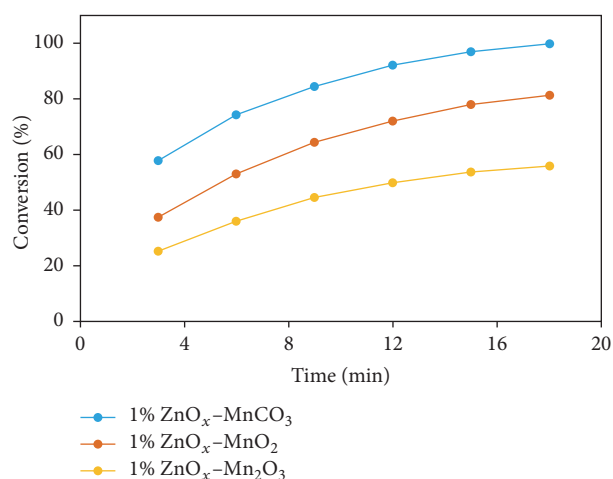


FIGURE 7: Graphical illustration of 1-phenylethanol oxidation using catalyst calcined at different calcination temperature.

60.14%, respectively. Additionally, the specific activity, TON, and TOF were found to decrease with increased ZnO_x content in the catalyst (Table 2, entries 3–5), although the selectivity towards acetophenone was more than 99% for all reactions. As illustrated in Figure 8, the ZnO_x NPs play a fundamental role in improving the catalytic performance for the selective oxidation of 1-phenylethanol. Moreover, as % ZnO_x increases the conversion of 1-phenylethanol decreases, probably due to the agglomeration of ZnO_x NPs in the catalyst surface or to a blocking of active sites as indicated by the results of the BET analysis. The results indicate that 1% $\text{ZnO}_x\text{-MnCO}_3$ catalyst was the best among all catalysts synthesized. Hence, we choose to use 1% $\text{ZnO}_x\text{-MnCO}_3$ in the further studies.

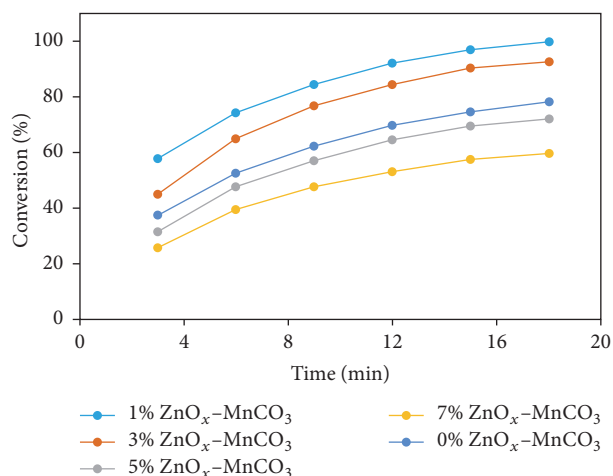


FIGURE 8: The effect of different weight % ZnO_x on the 1-phenylethanol oxidation.

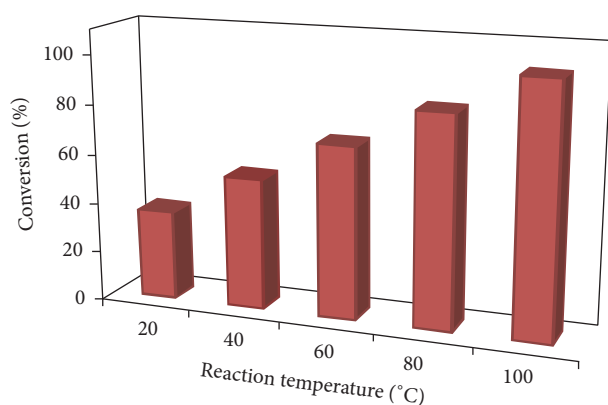


FIGURE 9: Catalytic performance of 1% ZnO_x-MnCO₃ catalyst as a function of reaction temperature.

3.8.3. Influence of Temperature. The effect of reaction temperature on the conversion of 1-phenylethanol and the acetophenone selectivity was investigated by considering five different temperatures in the range of 20–100°C. The results including alcohol conversion, specific activity, TON, TOF, and product selectivity have been summarized in Table 3 and plotted in Figure 9. The acetophenone selectivity was almost unchanged (>99%), whereas the conversion of 1-phenylethanol strongly depends on the reaction temperature. For instance, at low reaction temperature of 20°C, a relatively low alcohol conversion of 36.07% has been obtained (Table 3, entry 1). As expected, the high temperature contributed to a higher oxidation rate and led to the remarkable improvement of catalytic activity of the prepared catalyst. A full conversion of 1-phenylethanol was achieved at 100°C within relatively short reaction time (18 min) under identical reaction conditions (Table 3, entry 5). In addition, when the reaction temperature increased, the specific activity, TON, and TOF were also increased as shown in Table 3. Therefore, 100°C was chosen to be an optimum reaction temperature in this study to achieve highest catalytic performance.

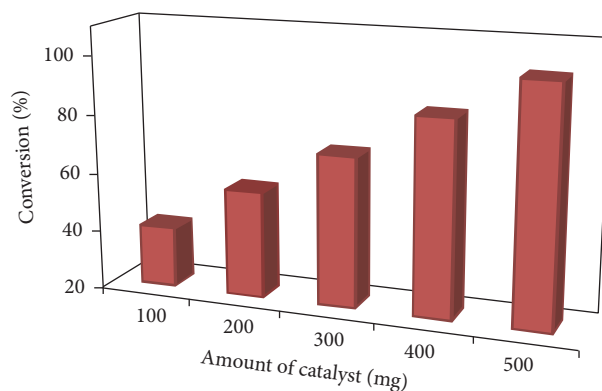


FIGURE 10: Catalytic activity of 1% ZnO_x-MnCO₃ catalyst as a function of catalyst amount.

3.8.4. Influence of Catalyst Amount. The 1-phenylethanol conversion and the selectivity of acetophenone using different catalyst amounts were also evaluated, and the results are illustrated in Table 4 and Figure 10. The oxidation reaction was carried out in presence of 100, 200, 300, 400, and 500 mg of 1% ZnO_x-MnCO₃ catalyst under the optimized reaction conditions. It is noteworthy that the catalytic activity of the as-synthesized catalyst is directly proportional to the catalyst amounts. According to Table 4, the alcohol conversion increased from 40.58% to 100% by increasing the catalyst amount from 100 to 500 mg within short reaction time (5 min), whereas the product selectivity was almost unchanged during all oxidation processes (above 99%). Moreover, a blank reaction has also been examined in the absence of the catalyst. It was found that no formation of acetophenone was obtained, indicating that the catalyst is necessary for the oxidation of 1-phenylethanol.

Furthermore, in order to show the superior catalytic activity of the present catalytic system, the effectiveness of our catalytic system has been compared with the ones already reported in the scientific literature in the oxidation of 1-phenylethanol (Table 5). Obviously, the as-synthesized 1% ZnO_x-MnCO₃ is the most efficient catalyst among all the listed catalysts. Herein, the prepared catalyst has been used for 1-phenylethanol oxidation and exhibited a full conversion and selectivity within extremely short reaction time of 5 min at 100°C and highest specific activity (48 mmol·g⁻¹·h⁻¹) compared to all other listed catalysts. In contrast, all listed catalysts take a very long reaction time to completely oxidize 1-phenylethanol and require higher reaction temperature. For instance, Hosseini-Sarvari et al. [76] have prepared Ag nanoparticles doped ZnO support (Ag/ZnO) and used it as a catalyst for selective oxidation of alcohols to their corresponding carbonyls. The nano Ag/ZnO catalyst provided 90% conversion of 1-phenylethanol and more than 99% selectivity of acetophenone along with 30 mmol·g⁻¹·h⁻¹ specific activity after long reaction time of 6 h at 100°C. In another example, Nepak and Darbha [70] reported liquid-phase selective alcohol oxidation over Au-Pd NPs doped in sodium titanate nanotubes (NaTNTs) as a catalyst. The Au-Pd/NaTNT catalyst exhibited 1-phenylethanol conversion of 84% and product

TABLE 5: A comparison between performance of our catalytic system and earlier reported catalysts for 1-phenylethanol oxidation.

Catalyst	Conv. (%)	Sel. (%)	T ($^{\circ}\text{C}$)	Time	Sp. activity ($\text{mmol}\cdot\text{g}^{-1}\cdot\text{h}^{-1}$)	Ref.
1% $\text{ZnO}_x\text{-MnCO}_3$	100	>99	100	5 min	48.0	This work
Cu/AlO(OH)	99	97	27	5 h	8.08	[66]
$\text{VO}_2\text{SO}_4/\text{TEMPO}$	99	96	80	2 h	37.78	[67]
SSDT	90	>99	reflux	1 h	1.8	[68]
Au/MgO	97	>99	130	2 h	19.4	[69]
Au-Pd/NaTNT	84	86	120	10 h	42.0	[70]
CdS-MTA	40	>99	5	1.5 h	0.60	[71]
Au-Pd/LDH	>99	>99	80	1.5 h	6.67	[72]
Au/TiO ₂	100	>99	110	24 h	0.83	[73]
$\text{Fe}(\text{NO}_3)_3\cdot 9\text{H}_2\text{O}/\text{ABNO}$	87	>99	RT	4 h	5.44	[74]
$\text{FeCl}_3\text{-imine@SiO}_2$	90	>99	80	6 h	3.26	[75]
Ag/ZnO	90	>99	100	6 h	30.0	[76]
CoTE4PyP-MT	92	89	70	2 h	30.67	[77]
Mn(III)-salen	46.9	>99	20	40 min	5.77	[78]
5 wt% Ir/TiO ₂	97	95	80	48 h	0.40	[79]
Ru/CaO-ZrO ₂	>99	>98	40	6 h	1.67	[80]
CeCrO ₃	100	100	90	6 h	15.15	[62]
Ru/Mg-LaO	96	>99	80	4 h	2.4	[81]
CoAl_2O_4	63.45	83.25	80	8 h	0.79	[34]
Fe_3O_4	76	>99	80	18 h	1.4	[82]

selectivity of about 86%, and the specific activity of this conversion was about $42\text{ mmol}\cdot\text{g}^{-1}\cdot\text{h}^{-1}$ within long reaction time of 10 h at higher reaction temperature of 120°C . As a result, the prepared 1% $\text{ZnO}_x\text{-MnCO}_3$ catalyst has been found to be the best choice for the alcohol oxidation.

3.9. Recycling Studies. The reusability of the catalyst has considerable importance from both commercial and academic point of view. In order to evaluate the recyclability and the stability, the oxidation of 1-phenylethanol was performed 5 times under optimum reaction conditions with the recycling of 1% $\text{ZnO}_x\text{-MnCO}_3$ catalyst and results are shown in Figure 11. After the first use of the catalyst in the oxidation of 1-phenylethanol to give acetophenone, the toluene was evaporated and fresh toluene was added and the mixture was filtered by centrifugation to recover the catalyst. The filtered catalyst was washed sequentially with toluene. The results revealed that the 1% $\text{ZnO}_x\text{-MnCO}_3$ catalyst was reused for at least 5 cycles with no appreciable decrease in its activity being observed and selectivity remained unchanged throughout all runs. During the five recycling reactions, the conversion of 1-phenylethanol decreased gradually from 100% to 92.37%, possibly due to the mass loss during the filtration method [92, 93]. Therefore, results indicate an excellent recyclability and stability of the as-prepared catalyst.

3.10. Oxidation of Different Types of Alcohols over 1% $\text{ZnO}_x\text{-MnCO}_3$ Catalyst. For evaluation of the catalyst capabilities, a variety of alcohols including secondary, benzylic aliphatic, primary allylic, and heteroatomic alcohols were subjected to oxidation with molecular O_2 under the optimized circumstances (Table 6, entries 1–26). The optimal

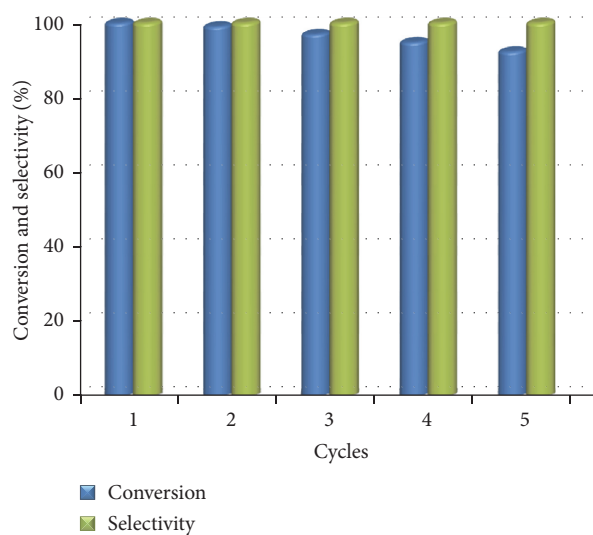


FIGURE 11: Recyclability of 1% $\text{ZnO}_x\text{-MnCO}_3$ for the aerial oxidation of 1-phenylethanol (reaction conditions: 2 mmol of 1-phenylethanol, calcination temperature at 300°C , oxygen with rate 20 mL/min, 0.5 g of catalyst, 10 mL of toluene, reaction temperature at 100°C , and 5 min of reaction time).

reaction conditions include 2 mmol of alcohol in 10 mL toluene with 20 mL/min oxygen flow rate and 100°C reaction temperature in presence of 1% $\text{ZnO}_x\text{-MnCO}_3$ catalyst (0.5 g) calcined at 300°C . The results are summarized in Table 6. The results showed that all secondary aromatic alcohols were selectively oxidized into their corresponding ketones with 100% convertibility under optimized circumstances (Table 6,

TABLE 6: Oxidation of different types of alcohols over 1% ZnO_x-MnCO₃ catalyst.^[a]

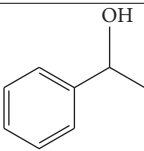
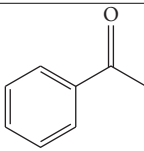
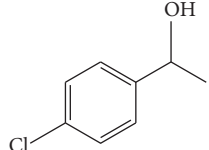
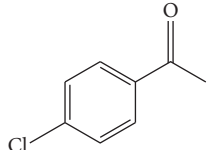
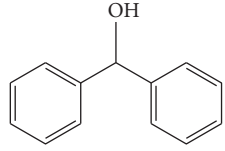
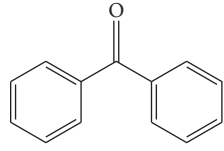
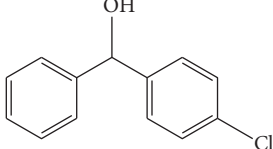
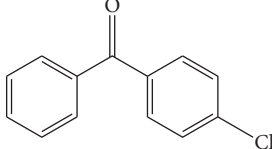
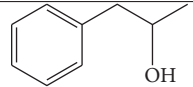
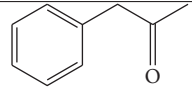
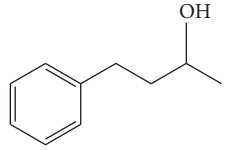
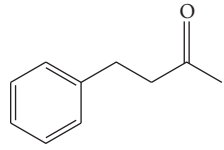
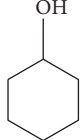
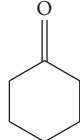
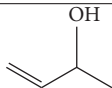
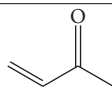
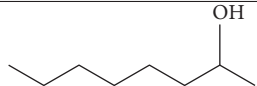
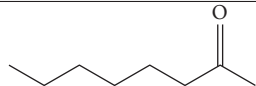
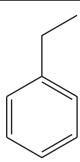
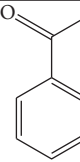
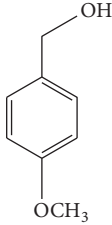
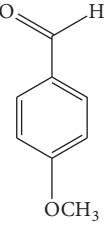
R. number	Reactants	Products	Time (min)	Conv. (%)	Sel. (%)
1			5	100	>99
2			8	100	>99
3			4	100	>99
4			6	100	>99
5			10	100	>99
6			13	100	>99
7			30	100	>99
8			80	100	>99
9			85	100	>99
10			4	100	>99
11			4	100	>99

TABLE 6: Continued.

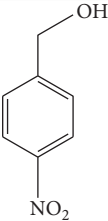
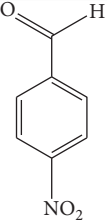
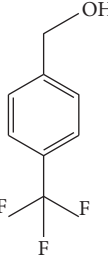
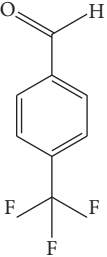
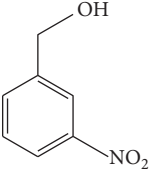
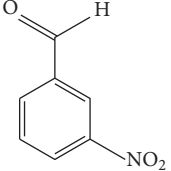
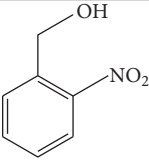
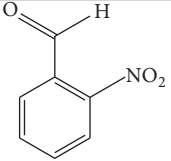
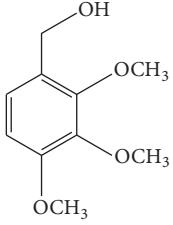
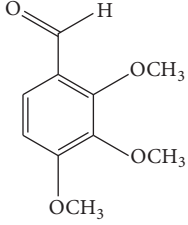
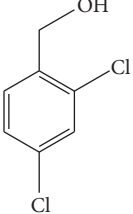
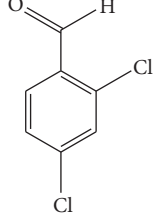
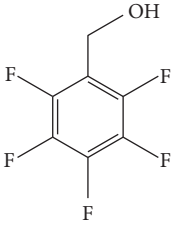
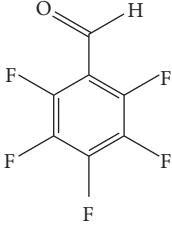
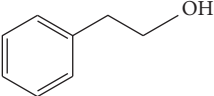
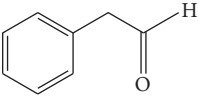
R. number	Reactants	Products	Time (min)	Conv. (%)	Sel. (%)
12			7	100	>99
13			8	100	>99
14			8	100	>99
15			11	100	>99
16			9	100	>99
17			12	100	>99
18			15	100	>99
19			10	100	>99

TABLE 6: Continued.

R. number	Reactants	Products	Time (min)	Conv. (%)	Sel. (%)
20			20	100	>99
21			7	100	>99
22			20	100	>99
23			35	100	>99
24			70	100	>99
25			75	100	>99
26			90	100	>99

^[a] Reaction conditions: 2 mmol of alcohol, 0.5 g of catalyst, calcination temperature at 300°C, oxygen with rate 20 mL/min, reaction temperature at 100°C, and 10 mL of toluene.

entries 1–6). Additionally, an excellent selectivity (above 99%) towards ketones has been obtained throughout all oxidation processes and no by-products were found in the reaction mixture. It is noteworthy that the benzhydrol was demonstrated to be the most reactive among all secondary aromatic alcohols and gave 100% conversion after 4 min, while the 4-chlorobenzhydrol gave 100% conversion after longer reaction time, maybe because 4-chlorobenzhydrol contains electron-withdrawing group that deactivate the phenyl ring by decreasing the electron density (Table 6, entries 3 and 4). Furthermore, 1-phenylethanol and its derivatives also afforded complete conversion and more than 99% selectivity in relatively short reaction times (Table 6, entries 1 and 2). Commonly, the oxidation of aliphatic alcohols is much more difficult than aromatic ones [94–96]. Indeed, our catalytic protocol was also found to be effective for oxidation of secondary aliphatic alcohols to their corresponding ketones under the similar reaction conditions (Table 6, entries 7–9).

As expected, it was necessary to increase reaction time, because the oxidation of secondary aliphatic alcohols is more difficult than secondary aromatic alcohols; for example, 2-octanol required relatively longer reaction time (85 min) for complete oxidation to 2-octanone (Table 6, entry 9).

In order to exploit the applicability of the present catalytic system and to generalize the scope of the oxidation process, the oxidation reaction has extended to various types of alcohol such as primary aromatic, allylic, heteroaromatic, and aliphatic alcohols. Generally, all primary aromatic alcohols could be oxidized rapidly to the corresponding aldehydes with complete conversions within very short reaction times (Table 6, entries 10–22). Moreover, more than 99% selectivity to corresponding aldehydes has been achieved in most of oxidation reactions and no other products were detected in the reaction mixture because no overoxidation to carboxylic acids occurred. The oxidation of the primary benzylic alcohols was strongly influenced by the electronic properties of

the substituents on the benzyl group. In general, the oxidation rate of aromatic alcohols with electron-releasing groups was relatively higher than that of alcohols with electron-withdrawing group [13, 97, 98]. For instance, oxidation of an aromatic alcohol containing electron-donating group such as 4-methoxybenzyl alcohol gave 100% conversion only in 4 min (Table 6, entry 11), while oxidation of alcohol bearing electron-withdrawing group like 4-(trifluoromethyl)benzyl alcohol afforded 100% conversion within longer reaction time (8 min) (Table 6, entry 13). On the other hand, *para*-substituted alcohols have higher activities relative to *ortho*- and *meta*-substituent, probably because the *para*-position has minimum steric hindrance compared to other positions [99, 100]. For an example, *para*-nitrobenzyl alcohol was fully oxidized into its corresponding aldehyde within 7 min (Table 6, entry 12), while *meta*- and *ortho*-nitrobenzyl alcohol were completely oxidized after longer times, 8 and 11 min, respectively (Table 6, entries 14 and 15). Steric hindrance is another essential factor that affects the rate of the oxidation processes; the bulky groups such as 4-CF₃, 2,4-DiCl, 2,3,4-TriOMe, and 2,3,4,5,6-pentafluoro attached to benzyl alcohol decrease the performance of the oxidation reaction, maybe because of the steric resistance that impedes the oxidation of the alcohols bearing bulky substituents (Table 6, entries 13, 16–18). Cinnamyl alcohol, an example of allylic alcohols, has been completely oxidized to cinnamaldehyde with more than 99% cinnamaldehyde selectivity within 7 min (Table 6, entry 21). A heteroaromatic alcohol such as furfuryl alcohol has been converted to furfural within 20 min, with complete conversion and product selectivity (Table 6, entry 22). Furthermore, compared to primary aromatic alcohols, the oxidation of primary aliphatic alcohols exhibited relatively low reactivity towards oxidation reaction (Table 6, entries 23–26). In this regard, the oxidation of cyclohexanemethanol, 5-Hexen-1-ol, octan-1-ol, and citronellol into their corresponding aldehydes occurs in slightly longer reaction times (Table 6, entries 23–26). As a result, it can be said that the aerobic oxidation of alcohols catalyzed by 1% ZnO_x-MnCO₃ has been affected by two factors, electronic and steric effects.

4. Conclusions

In conclusion, ZnO_x NPs doped MnCO₃ was found to be an efficient catalyst towards the catalytic oxidation of alcohols to carbonyls with molecular O₂ as a clean oxidant without using any additive or base. Interestingly, the ZnO_x NPs play a fundamental role in the catalytic performance because the oxidation rate has remarkably improved after doping ZnO_x NPs on MnCO₃. A complete 1-phenylethanol conversion can be accomplished within extremely short reaction time of only 5 min along with 48 mmol·g⁻¹·h⁻¹ specific activity and 390.6 TOF. The obtained specific activity is much higher than that reported in earlier literatures. Additionally, wide range of benzylic, aliphatic, allylic, primary, and secondary alcohols has been studied for aerobic oxidation into their corresponding aldehydes and ketones with excellent alcohols conversion within relatively short reaction times under mild reaction conditions. Furthermore, the very high product selectivity (>99%) has been achieved for most of alcohols

used in this work. The as-prepared catalyst can be recycled and reused for five times without any obvious loss of catalytic activity and the selectivity remained almost unchanged. This catalytic system offers several advantages including complete alcohol conversions and extremely high specific activities and selectivity towards products in extremely short reaction times by using ecofriendly, low cost, selective, facile synthesis, and reusable heterogeneous catalyst will make this system useful and applicable for the selective oxidation of alcohols.

Conflicts of Interest

The authors declare that they have no conflicts of interest.

Acknowledgments

The authors extend their appreciation to the Deanship of Scientific Research at King Saud University for funding this work through the Research Group Project no. RG-1436-032.

References

- [1] G.-J. ten Brink, I. W. C. E. Arends, and R. A. Sheldon, "Green, catalytic oxidation of alcohols in water," *Science*, vol. 287, no. 5458, pp. 1636–1639, 2000.
- [2] M. Pagliaro, S. Campestrini, and R. Ciriminna, "Ru-based oxidation catalysis," *Chemical Society Reviews*, vol. 34, no. 10, pp. 837–845, 2005.
- [3] K. Mori, T. Hara, T. Mizugaki, K. Ebitani, and K. Kaneda, "Hydroxyapatite-supported palladium nanoclusters: a highly active heterogeneous catalyst for selective oxidation of alcohols by use of molecular oxygen," *Journal of the American Chemical Society*, vol. 126, no. 34, pp. 10657–10666, 2004.
- [4] I. E. Markó, P. R. Giles, M. Tsukazaki, S. M. Brown, and C. J. Urch, "Copper-catalyzed oxidation of alcohols to aldehydes and ketones: an efficient, aerobic alternative," *Science*, vol. 274, no. 5295, pp. 2044–2046, 1996.
- [5] T. Mallat and A. Baiker, "Oxidation of alcohols with molecular oxygen on solid catalysts," *Chemical Reviews*, vol. 104, no. 6, pp. 3037–3058, 2004.
- [6] J. Ahmad, P. Figiel, M. Räisänen, M. Leskelä, and T. Repo, "Aerobic oxidation of benzylic alcohols with bis(3,5-di-*tert*-butylsalicylaldimine)copper(II) complexes," *Applied Catalysis A: General*, vol. 371, no. 1-2, pp. 17–21, 2009.
- [7] C. Parmeggiani and F. Cardona, "Transition metal based catalysts in the aerobic oxidation of alcohols," *Green Chemistry*, vol. 14, no. 3, pp. 547–564, 2012.
- [8] Z. Guo, B. Liu, Q. Zhang, W. Deng, Y. Wang, and Y. Yang, "Recent advances in heterogeneous selective oxidation catalysis for sustainable chemistry," *Chemical Society Reviews*, vol. 43, no. 10, pp. 3480–3524, 2014.
- [9] G. Palmisano, E. García-López, G. Marci et al., "Advances in selective conversions by heterogeneous photocatalysis," *Chemical Communications*, vol. 46, no. 38, pp. 7074–7089, 2010.
- [10] S. Higashimoto, N. Suetsugu, M. Azuma, H. Ohue, and Y. Sakata, "Efficient and selective oxidation of benzylic alcohol by O₂ into corresponding aldehydes on a TiO₂ photocatalyst under visible light irradiation: effect of phenyl-ring substitution on the photocatalytic activity," *Journal of Catalysis*, vol. 274, no. 1, pp. 76–83, 2010.

- [11] M. Zhang, Q. Wang, C. Chen, L. Zang, W. Ma, and J. Zhao, "Oxygen atom transfer in the photocatalytic oxidation of alcohols by TiO_2 : oxygen isotope studies," *Angewandte Chemie*, vol. 121, no. 33, pp. 6197–6200, 2009.
- [12] S. Yurdakal, G. Palmisano, V. Loddo, V. Augugliaro, and L. Palmisano, "Nanostructured rutile TiO_2 for selective photocatalytic oxidation of aromatic alcohols to aldehydes in water," *Journal of the American Chemical Society*, vol. 130, no. 5, pp. 1568–1569, 2008.
- [13] D. I. Enache, J. K. Edwards, P. Landon et al., "Solvent-free oxidation of primary alcohols to aldehydes using Au-Pd/ TiO_2 catalyst," *Science*, vol. 311, no. 5759, pp. 362–365, 2006.
- [14] M. M. Dell'Anna, M. Mali, P. Mastrorilli, P. Cotugno, and A. Monopoli, "Oxidation of benzyl alcohols to aldehydes and ketones under air in water using a polymer supported palladium catalyst," *Journal of Molecular Catalysis A: Chemical*, vol. 386, pp. 114–119, 2014.
- [15] B.-Z. Zhan and A. Thompson, "Recent developments in the aerobic oxidation of alcohols," *Tetrahedron*, vol. 60, no. 13, pp. 2917–2935, 2004.
- [16] J. Yu, J. Li, H. Wei, J. Zheng, H. Su, and X. Wang, "Hydrotalcite-supported gold catalysts for a selective aerobic oxidation of benzyl alcohol driven by visible light," *Journal of Molecular Catalysis A: Chemical*, vol. 395, pp. 128–136, 2014.
- [17] Y. Li, Y. Gao, and C. Yang, "A facile and efficient synthesis of polystyrene/gold-platinum composite particles and their application for aerobic oxidation of alcohols in water," *Chemical Communications*, vol. 51, no. 36, pp. 7721–7724, 2015.
- [18] S. Alabbad, S. F. Adil, M. E. Assal, M. Khan, A. Alwarthan, and M. R. H. Siddiqui, "Gold & silver nanoparticles supported on manganese oxide: synthesis, characterization and catalytic studies for selective oxidation of benzyl alcohol," *Arabian Journal of Chemistry*, vol. 7, no. 6, pp. 1192–1198, 2014.
- [19] R. H. Adnan, G. G. Andersson, M. I. J. Polson, G. F. Metha, and V. B. Golovko, "Factors influencing the catalytic oxidation of benzyl alcohol using supported phosphine-capped gold nanoparticles," *Catalysis Science and Technology*, vol. 5, no. 2, pp. 1323–1333, 2015.
- [20] T. Wang, X. Yuan, S. Li, L. Zeng, and J. Gong, " CeO_2 -modified Au@SBA-15 nanocatalysts for liquid-phase selective oxidation of benzyl alcohol," *Nanoscale*, vol. 7, no. 17, pp. 7593–7602, 2015.
- [21] Y. Yan, X. Jia, and Y. Yang, "Palladium nanoparticles supported on CNT functionalized by rare-earth oxides for solvent-free aerobic oxidation of benzyl alcohol," *Catalysis Today*, vol. 259, pp. 292–302, 2014.
- [22] Y. Hong, X. Yan, X. Liao et al., "Platinum nanoparticles supported on Ca(Mg)-zeolites for efficient room-temperature alcohol oxidation under aqueous conditions," *Chemical Communications*, vol. 50, no. 68, pp. 9679–9682, 2014.
- [23] T. Wang, H. Shou, Y. Kou, and H. Liu, "Base-free aqueous-phase oxidation of non-activated alcohols with molecular oxygen on soluble Pt nanoparticles," *Green Chemistry*, vol. 11, no. 4, pp. 562–568, 2009.
- [24] K. Kon, S. M. A. Hakim Siddiki, and K.-I. Shimizu, "Size- and support-dependent Pt nanocluster catalysis for oxidant-free dehydrogenation of alcohols," *Journal of Catalysis*, vol. 304, pp. 63–71, 2013.
- [25] Z.-W. Yang, X. Zhao, T.-J. Li et al., "Catalytic properties of palygorskite supported Ru and Pd for efficient oxidation of alcohols," *Catalysis Communications*, vol. 65, pp. 34–40, 2015.
- [26] D. Canseco-Gonzalez and M. Albrecht, "Wingtip substituents tailor the catalytic activity of ruthenium triazolylidene complexes in base-free alcohol oxidation," *Dalton Transactions*, vol. 42, no. 20, pp. 7424–7432, 2013.
- [27] A. Wusiman and C.-D. Lu, "Selective oxidation of benzylic, allylic and propargylic alcohols using dirhodium(II) tetraamidinate as catalyst and aqueous tert-butyl hydroperoxide as oxidant," *Applied Organometallic Chemistry*, vol. 29, no. 4, pp. 254–258, 2015.
- [28] J. Olguín, H. Müller-Bunz, and M. Albrecht, "Springloaded porphyrin NHC hybrid rhodium(III) complexes: carbene dissociation and oxidation catalysis," *Chemical Communications*, vol. 50, no. 26, pp. 3488–3490, 2014.
- [29] M. Xie, X. Dai, S. Meng, X. Fu, and S. Chen, "Selective oxidation of aromatic alcohols to corresponding aromatic aldehydes using In_2S_3 microsphere catalyst under visible light irradiation," *Chemical Engineering Journal*, vol. 245, pp. 107–116, 2014.
- [30] Q. Cao, L. M. Dornan, L. Rogan, N. L. Hughes, and M. J. Muldoon, "Aerobic oxidation catalysis with stable radicals," *Chemical Communications*, vol. 50, no. 35, pp. 4524–4543, 2014.
- [31] P. Cruz, Y. Pérez, I. Del Hierro, and M. Fajardo, "Copper, copper oxide nanoparticles and copper complexes supported on mesoporous SBA-15 as catalysts in the selective oxidation of benzyl alcohol in aqueous phase," *Microporous and Mesoporous Materials*, vol. 220, pp. 136–147, 2016.
- [32] R. Ali, M. E. Assal, and A. Al-Warthan, "Selective oxidation of benzylic alcohols with molecular oxygen catalyzed by copper-manganese oxide nanoparticles," *Asian Journal of Chemistry*, vol. 25, no. 9, article 4815, 2013.
- [33] S. M. Seyedi, R. Sandarooms, and G. H. Zohuri, "Novel cobalt(II) complexes of amino acids-Schiff bases catalyzed aerobic oxidation of various alcohols to ketones and aldehyde," *Chinese Chemical Letters*, vol. 21, no. 11, pp. 1303–1306, 2010.
- [34] C. Ragupathi, J. Judith Vijaya, S. Narayanan, S. K. Jesudoss, and L. John Kennedy, "Highly selective oxidation of benzyl alcohol to benzaldehyde with hydrogen peroxide by cobalt aluminate catalysis: a comparison of conventional and microwave methods," *Ceramics International*, vol. 41, no. 2, pp. 2069–2080, 2015.
- [35] S. R. Ali, P. Chandra, M. Latwal, S. K. Jain, V. K. Bansal, and S. P. Singh, "Synthesis of nickel hexacyanoferrate nanoparticles and their potential as heterogeneous catalysts for the solvent-free oxidation of benzyl alcohol," *Chinese Journal of Catalysis*, vol. 32, no. 11–12, pp. 1844–1849, 2011.
- [36] A. R. Hajipour, H. Karimi, and A. Koohi, "Selective oxidation of alcohols over nickel zirconium phosphate," *Chinese Journal of Catalysis*, vol. 36, no. 7, pp. 1109–1116, 2015.
- [37] H.-B. Ji, T.-T. Wang, M.-Y. Zhang, Q.-L. Chen, and X.-N. Gao, "Green oxidation of alcohols by a reusable nickel catalyst in the presence of molecular oxygen," *Reaction Kinetics and Catalysis Letters*, vol. 90, no. 2, pp. 251–257, 2007.
- [38] R. Naik, A. Nizam, A. Siddekha, and M. A. Pasha, "An efficient sonochemical oxidation of benzyl alcohols into benzaldehydes by $\text{FeCl}_3/\text{HNO}_3$ in acetone," *Ultrasonics Sonochemistry*, vol. 18, no. 5, pp. 1124–1127, 2011.
- [39] R. Cang, B. Lu, X. Li, R. Niu, J. Zhao, and Q. Cai, "Iron-chloride ionic liquid immobilized on SBA-15 for solvent-free oxidation of benzyl alcohol to benzaldehyde with H_2O_2 ," *Chemical Engineering Science*, vol. 137, pp. 268–275, 2015.
- [40] G. C. Behera and K. M. Parida, "Liquid phase catalytic oxidation of benzyl alcohol to benzaldehyde over vanadium phosphate catalyst," *Applied Catalysis A: General*, vol. 413–414, pp. 245–253, 2012.

- [41] S. F. Adil, M. E. Assal, M. Khan, A. Al-Warthan, and M. H. Rafiq Siddiqui, "Nano silver-doped manganese oxide as catalyst for oxidation of benzyl alcohol and its derivatives: synthesis, characterisation, thermal study and evaluation of catalytic properties," *Oxidation Communications*, vol. 36, no. 3, pp. 778–791, 2013.
- [42] M. Deng, G. Zhao, Q. Xue, L. Chen, and Y. Lu, "Microfibrillar-structured silver catalyst for low-temperature gas-phase selective oxidation of benzyl alcohol," *Applied Catalysis B: Environmental*, vol. 99, no. 1-2, pp. 222–228, 2010.
- [43] N. Noshiranzadeh, R. Bikas, K. Ślepokura, M. Mayeli, and T. Lis, "Synthesis, characterization and catalytic activity of new Cr(III) complex in oxidation of primary alcohols to aldehydes," *Inorganica Chimica Acta*, vol. 421, pp. 176–182, 2014.
- [44] P. S. N. Rao, K. T. V. Rao, P. S. Sai Prasad, and N. Lingaiah, "The role of vanadia for the selective oxidation of benzyl alcohol over heteropolymolybdate supported on alumina," *Chinese Journal of Catalysis*, vol. 32, no. 11, pp. 1719–1726, 2011.
- [45] A. V. Biradar, M. K. Dongare, and S. B. Umbarkar, "Selective oxidation of aromatic primary alcohols to aldehydes using molybdenum acetylido-oxo-peroxo complex as catalyst," *Tetrahedron Letters*, vol. 50, no. 24, pp. 2885–2888, 2009.
- [46] S. C. A. Sousa, J. R. Bernardo, P. R. Florindo, and A. C. Fernandes, "Efficient and selective oxidation of alcohols catalyzed by oxo-rhenium complexes," *Catalysis Communications*, vol. 40, pp. 134–138, 2013.
- [47] T. W. Goh, C. Xiao, R. V. Maligal-Ganesh, X. Li, and W. Huang, "Utilizing mixed-linker zirconium based metal-organic frameworks to enhance the visible light photocatalytic oxidation of alcohol," *Chemical Engineering Science*, vol. 124, pp. 45–51, 2015.
- [48] M. R. H. Siddiqui, I. Warad, S. F. Adil, R. M. Mahfouz, and A. Al-Arifi, "Nano-gold supported nickel manganese oxide: synthesis, characterisation and evaluation as oxidation catalyst," *Oxidation Communications*, vol. 35, no. 2, article 476, 2012.
- [49] S. F. Adil, S. Alabbad, M. Kuniyil et al., "Vanadia supported on nickel manganese oxide nanocatalysts for the catalytic oxidation of aromatic alcohols," *Nanoscale Research Letters*, vol. 10, no. 1, article 52, 2015.
- [50] Q. Tang, X. Gong, P. Zhao, Y. Chen, and Y. Yang, "Copper-manganese oxide catalysts supported on alumina: physico-chemical features and catalytic performances in the aerobic oxidation of benzyl alcohol," *Applied Catalysis A: General*, vol. 389, no. 1-2, pp. 101–107, 2010.
- [51] F. Arena, B. Gumina, A. F. Lombardo et al., "Nanostructured MnO_x catalysts in the liquid phase selective oxidation of benzyl alcohol with oxygen: part I. Effects of Ce and Fe addition on structure and reactivity," *Applied Catalysis B: Environmental*, vol. 162, pp. 260–267, 2015.
- [52] M. Yang, Q. Ling, R. Rao et al., " Mn_3O_4 -NiO-Ni/CNTs catalysts prepared by spontaneous redox at high temperature and their superior catalytic performance in selective oxidation of benzyl alcohol," *Journal of Molecular Catalysis A: Chemical*, vol. 380, pp. 61–69, 2013.
- [53] Y. Chen, H. Zheng, Z. Guo et al., "Pd catalysts supported on MnCeO_x mixed oxides and their catalytic application in solvent-free aerobic oxidation of benzyl alcohol: support composition and structure sensitivity," *Journal of Catalysis*, vol. 283, no. 1, pp. 34–44, 2011.
- [54] S. Mandal, C. Santra, K. K. Bando et al., "Aerobic oxidation of benzyl alcohol over mesoporous Mn-doped ceria supported Au nanoparticle catalyst," *Journal of Molecular Catalysis A: Chemical*, vol. 378, pp. 47–56, 2013.
- [55] M. Yang, Q. Ling, H. Yang, C. Li, and A. Zhang, "Enhanced catalytic activity of K-birnessite MnO_2 confined in carbon nanotubes for selective oxidation of benzyl alcohol," *Catalysis Communications*, vol. 46, pp. 238–241, 2014.
- [56] V. Mahdavi and M. Mardani, "Preparation of manganese oxide immobilized on SBA-15 by atomic layer deposition as an efficient and reusable catalyst for selective oxidation of benzyl alcohol in the liquid phase," *Materials Chemistry and Physics*, vol. 155, pp. 136–146, 2015.
- [57] T. J. Clarke, S. A. Kondrat, and S. H. Taylor, "Total oxidation of naphthalene using copper manganese oxide catalysts," *Catalysis Today*, vol. 258, pp. 610–615, 2015.
- [58] X. Guo, J. Li, and R. Zhou, "Catalytic performance of manganese doped CuO-CeO_2 catalysts for selective oxidation of CO in hydrogen-rich gas," *Fuel*, vol. 163, pp. 56–64, 2016.
- [59] M. Tepluchin, S. Kureti, M. Casapu, E. Ogel, S. Mangold, and J.-D. Grunwaldt, "Study on the hydrothermal and SO_2 stability of Al_2O_3 -supported manganese and iron oxide catalysts for lean CO oxidation," *Catalysis Today*, vol. 258, pp. 498–506, 2015.
- [60] S. C. Kim, Y.-K. Park, and J. W. Nah, "Property of a highly active bimetallic catalyst based on a supported manganese oxide for the complete oxidation of toluene," *Powder Technology*, vol. 266, pp. 292–298, 2014.
- [61] M. Piumetti, D. Fino, and N. Russo, "Mesoporous manganese oxides prepared by solution combustion synthesis as catalysts for the total oxidation of VOCs," *Applied Catalysis B: Environmental*, vol. 163, pp. 277–287, 2015.
- [62] Z. Feng, Y. Xie, F. Hao, P. Liu, and H. Luo, "Catalytic oxidation of cyclohexane to KA oil by zinc oxide supported manganese 5,10,15,20-tetrakis(4-nitrophenyl)porphyrin," *Journal of Molecular Catalysis A: Chemical*, vol. 410, pp. 221–225, 2015.
- [63] A. S. Burange, S. R. Kale, and R. V. Jayaram, "Oxidation of alkyl aromatics to ketones by tert-butyl hydroperoxide on manganese dioxide catalyst," *Tetrahedron Letters*, vol. 53, no. 24, pp. 2989–2992, 2012.
- [64] W. H. Yu, C. H. Zhou, D. S. Tong, and T. N. Xu, "Aerobic oxidation of 4-tert-butyltoluene over cobalt and manganese supported hexagonal mesoporous silicas as heterogeneous catalysts," *Journal of Molecular Catalysis A: Chemical*, vol. 365, pp. 194–202, 2012.
- [65] J. Pei, X. Han, and Y. Lu, "Performance and kinetics of catalytic oxidation of formaldehyde over copper manganese oxide catalyst," *Building and Environment*, vol. 84, pp. 134–141, 2015.
- [66] S. G. Babu, P. A. Priyadarsini, and R. Karvembu, "Copper on boehmite: a simple, selective, efficient and reusable heterogeneous catalyst for oxidation of alcohols with periodic acid in water at room temperature," *Applied Catalysis A: General*, vol. 392, no. 1-2, pp. 218–224, 2011.
- [67] Z. Du, J. Ma, H. Ma, M. Wang, Y. Huang, and J. Xu, "Vanadyl sulfate: a simple catalyst for oxidation of alcohols with molecular oxygen in combination with 2,2,6,6-tetramethyl-piperidyl-1-oxyl," *Catalysis Communications*, vol. 11, no. 8, pp. 732–735, 2010.
- [68] F. M. Moghaddam, N. Masoud, B. K. Foroushani, S. Saryazdi, N. Ghonouei, and E. Daemi, "Silica-supported DABCO-tribromide: a recoverable reagent for oxidation of alcohols to the corresponding carbonyl compounds," *Scientia Iranica*, vol. 20, no. 3, pp. 598–602, 2013.
- [69] V. V. Costa, M. Estrada, Y. Demidova et al., "Gold nanoparticles supported on magnesium oxide as catalysts for the aerobic oxidation of alcohols under alkali-free conditions," *Journal of Catalysis*, vol. 292, pp. 148–156, 2012.

- [70] D. Nepak and S. Darbha, "Selective aerobic oxidation of alcohols over Au-Pd/sodium titanate nanotubes," *Catalysis Communications*, vol. 58, pp. 149–153, 2015.
- [71] I. Tamiolakis, I. N. Lykakis, and G. S. Armatas, "Mesoporous CdS-sensitized TiO₂ nanoparticle assemblies with enhanced photocatalytic properties: selective aerobic oxidation of benzyl alcohols," *Catalysis Today*, vol. 250, pp. 180–186, 2015.
- [72] Y. Shi, H. Yang, X. Zhao et al., "Au-Pd nanoparticles on layered double hydroxide: highly active catalyst for aerobic oxidation of alcohols in aqueous phase," *Catalysis Communications*, vol. 18, pp. 142–146, 2012.
- [73] F. Vindigni, S. Dughera, F. Armigliato, and A. Chiorino, "Aerobic oxidation of alcohols on Au/TiO₂ catalyst: new insights on the role of active sites in the oxidation of primary and secondary alcohols," *Monatshefte für Chemie*, vol. 147, no. 2, pp. 391–403, 2016.
- [74] L. Wang, S. Shang, G. Li, L. Ren, Y. Lv, and S. Gao, "Iron/ABNO-catalyzed aerobic oxidation of alcohols to aldehydes and ketones under ambient atmosphere," *Journal of Organic Chemistry*, vol. 81, no. 5, pp. 2189–2193, 2016.
- [75] D. Sahu, A. R. Silva, and P. Das, "A novel iron(III)-based heterogeneous catalyst for aqueous oxidation of alcohols using molecular oxygen," *RSC Advances*, vol. 5, no. 96, pp. 78553–78560, 2015.
- [76] M. Hosseini-Sarvari, T. Ataee-Kachouei, and F. Moeini, "A novel and active catalyst Ag/ZnO for oxidant-free dehydrogenation of alcohols," *Materials Research Bulletin*, vol. 72, pp. 98–105, 2015.
- [77] X. Zhou and H. Ji, "Cobalt porphyrin immobilized on montmorillonite: a highly efficient and reusable catalyst for aerobic oxidation of alcohols to carbonyl compounds," *Chinese Journal of Catalysis*, vol. 33, no. 11–12, pp. 1906–1912, 2012.
- [78] Y. Zhang, Q. Zhou, W. Ma, and J. Zhao, "Enantioselective oxidation of racemic secondary alcohols catalyzed by chiral Mn(III)-salen complex with sodium hypochlorite as oxidant," *Catalysis Communications*, vol. 45, pp. 114–117, 2014.
- [79] A. Yoshida, Y. Takahashi, T. Ikeda, K. Azemoto, and S. Naito, "Catalytic oxidation of aromatic alcohols and alkylarenes with molecular oxygen over Ir/TiO₂," *Catalysis Today*, vol. 164, no. 1, pp. 332–335, 2011.
- [80] T. Yasu-eda, S. Kitamura, N.-O. Ikenaga, T. Miyake, and T. Suzuki, "Selective oxidation of alcohols with molecular oxygen over Ru/CaO-ZrO₂ catalyst," *Journal of Molecular Catalysis A: Chemical*, vol. 323, no. 1–2, pp. 7–15, 2010.
- [81] M. L. Kantam, R. S. Reddy, U. Pal et al., "Ruthenium/magnesium-lanthanum mixed oxide: an efficient reusable catalyst for oxidation of alcohols by using molecular oxygen," *Journal of Molecular Catalysis A: Chemical*, vol. 359, pp. 1–7, 2012.
- [82] M. Shaikh, M. Satanami, and K. V. S. Ranganath, "Efficient aerobic oxidation of alcohols using magnetically recoverable catalysts," *Catalysis Communications*, vol. 54, pp. 91–93, 2014.
- [83] W. Gac, "The influence of silver on the structural, redox and catalytic properties of the cryptomelane-type manganese oxides in the low-temperature CO oxidation reaction," *Applied Catalysis B: Environmental*, vol. 75, no. 1–2, pp. 107–117, 2007.
- [84] R. K. Kunkalekar and A. V. Salker, "Low temperature carbon monoxide oxidation over nanosized silver doped manganese dioxide catalysts," *Catalysis Communications*, vol. 12, no. 3, pp. 193–196, 2010.
- [85] L. Chen, B. Sun, X. Wang, F. Qiao, and S. Ai, "2D ultrathin nanosheets of Co-Al layered double hydroxides prepared in l-asparagine solution: enhanced peroxidase-like activity and colorimetric detection of glucose," *Journal of Materials Chemistry B*, vol. 1, no. 17, pp. 2268–2274, 2013.
- [86] A. C. Tas, "Calcium metal to synthesize amorphous or cryptocrystalline calcium phosphates," *Materials Science and Engineering C*, vol. 32, no. 5, pp. 1097–1106, 2012.
- [87] D. P. Dubal, D. S. Dhawale, R. R. Salunkhe, S. M. Pawar, and C. D. Lokhande, "A novel chemical synthesis and characterization of Mn₃O₄ thin films for supercapacitor application," *Applied Surface Science*, vol. 256, no. 14, pp. 4411–4416, 2010.
- [88] E. N. Maslen, V. A. Streltsov, N. R. Streltsova, and N. Ishizawa, "Electron density and optical anisotropy in rhombohedral carbonates. III. Synchrotron X-ray studies of CaCO₃, MgCO₃ and MnCO₃," *Acta Crystallographica Section B*, vol. 51, no. 6, pp. 929–939, 1995.
- [89] C. Zhu, G. Saito, and T. Akiyama, "A new CaCO₃-template method to synthesize nanoporous manganese oxide hollow structures and their transformation to high-performance LiMn₂O₄ cathodes for lithium-ion batteries," *Journal of Materials Chemistry A*, vol. 1, no. 24, pp. 7077–7082, 2013.
- [90] G. Zhan, Y. Hong, V. T. Mbah et al., "Bimetallic Au-Pd/MgO as efficient catalysts for aerobic oxidation of benzyl alcohol: a green bio-reducing preparation method," *Applied Catalysis A: General*, vol. 439–440, pp. 179–186, 2012.
- [91] G. Wu, Y. Gao, F. Ma et al., "Catalytic oxidation of benzyl alcohol over manganese oxide supported on MCM-41 zeolite," *Chemical Engineering Journal*, vol. 271, pp. 14–22, 2015.
- [92] E. G. Rodrigues, J. J. Delgado, X. Chen, M. F. R. Pereira, and J. J. M. Órfão, "Selective oxidation of glycerol catalyzed by gold supported on multiwalled carbon nanotubes with different surface chemistries," *Industrial and Engineering Chemistry Research*, vol. 51, no. 49, pp. 15884–15894, 2012.
- [93] X. Yu, Y. Huo, J. Yang, S. Chang, Y. Ma, and W. Huang, "Reduced graphene oxide supported Au nanoparticles as an efficient catalyst for aerobic oxidation of benzyl alcohol," *Applied Surface Science*, vol. 280, pp. 450–455, 2013.
- [94] E. Assady, B. Yadollahi, M. Riahi Farsani, and M. Moghadam, "Zinc polyoxometalate on activated carbon: an efficient catalyst for selective oxidation of alcohols with hydrogen peroxide," *Applied Organometallic Chemistry*, vol. 29, no. 8, pp. 561–565, 2015.
- [95] S. Hasannia and B. Yadollahi, "Zn-Al LDH nanostructures pillared by Fe substituted Keggin type polyoxometalate: synthesis, characterization and catalytic effect in green oxidation of alcohols," *Polyhedron*, vol. 99, pp. 260–265, 2015.
- [96] J. Albadi, A. Alihoseinzadeh, and A. Razeghi, "Novel metal oxide nanocomposite of Au/CuO-ZnO for recyclable catalytic aerobic oxidation of alcohols in water," *Catalysis Communications*, vol. 49, pp. 1–5, 2014.
- [97] Z. Nadealian, V. Mirkhani, B. Yadollahi, M. Moghadam, S. Tangestaninejad, and I. Mohammadpoor-Baltork, "Selective oxidation of alcohols to aldehydes using inorganic-organic hybrid catalyst based on zinc substituted polyoxometalate and ionic liquid," *Journal of Coordination Chemistry*, vol. 65, no. 6, pp. 1071–1081, 2012.
- [98] K. P. Peterson and R. C. Larock, "Palladium-catalyzed oxidation of primary and secondary allylic and benzylic alcohols," *Journal of Organic Chemistry*, vol. 63, no. 10, pp. 3185–3189, 1998.

- [99] M. M. Kadam, K. B. Dhopte, N. Jha, V. G. Gaikar, and P. R. Nemade, "Synthesis, characterization and application of γ - MnO_2 /graphene oxide for the selective aerobic oxidation of benzyl alcohols to corresponding carbonyl compounds," *New Journal of Chemistry*, vol. 40, no. 2, pp. 1436–1442, 2016.
- [100] M. Heidari-Golafzani, M. Rabbani, R. Rahimi, and A. Azad, "Catalytic oxidation of primary and secondary alcohols over a novel TCPP/Zn- Fe_2O_4 @ZnO catalyst," *RSC Advances*, vol. 5, no. 121, pp. 99640–99645, 2015.

